

b

Two-dimension plasma expansions with anisotropic pressure

Yongsheng Huang,^{1,2,*} Yuanjie Bi,^{1,2} Xiaojiao Duan,¹

Naiyan Wang,¹ Xiuzhang Tang,¹ and Zhe Gao²

¹*China Institute of Atomic Energy, Beijing 102413, China.*

²*Department of Engineering Physics, Tsinghua University, Beijing 100084, China.*

(Dated: November 6, 2018)

Abstract

A two-dimension self-similar solution is proposed for a plasma expansion with anisotropic pressure. With the solution, it depends on the relationship between the ratio of the longitudinal and the transverse temperature of the plasma, κ^2 and the electron-ion mass ratio, μ , that the plasma front is composed by a part of hyperbolic (or a plane) and a small pointed projection at the center or a part of an ellipse. Zhang and coworkers's experiments (PRL, 99, 167602 (2007)) support our results for $\kappa^2 \in (\tau, 1]$. For $\kappa^2 \leq \tau$, there is an anomalous high-energy plasma emission at the angle of near 90° due to longitudinal Coulomb explosion.

PACS numbers: 52.38.Kd, 41.75.Jv, 52.40.Kh, 52.65.-y

*Electronic address: huangyongs@gmail.com

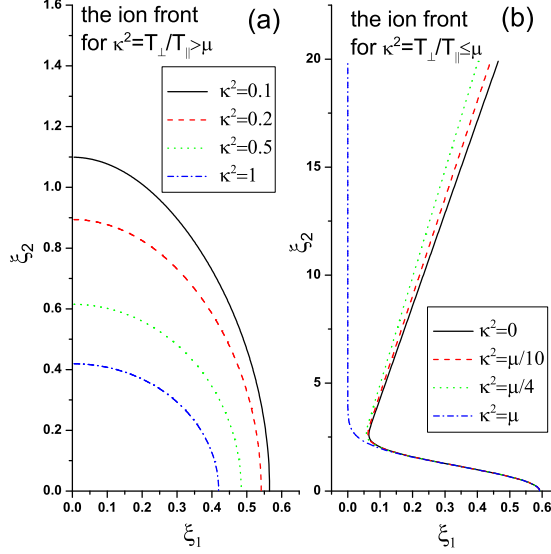


FIG. 1: (Color online) (ξ_1, ξ_2) at the ion front for different κ^2 , the ratio of T_\perp and T_\parallel , which is compared with $\mu = Zm_e/m_i$, the mass ratio of electron and ion for $\phi^0 = 1$ and $C_0 = 0$ in Eq. (2). Figure 1(a) and (b) are obtained from the solutions of Eq. (2). In Figure 1(a), $\kappa^2 = T_\perp/T_\parallel > \mu$. In these cases, the curve of the ion front is a part of an ellipse, especially, a cycle for $\kappa^2 = 1$. The major axis of the ellipse is in the lower-temperature direction. In Figure 1 (b), $\kappa^2 = T_\perp/T_\parallel \leq \mu$. In this case, the ion front contains two parts. For $\xi_2 \geq 2.5$, the ion front is a part of a hyperbola or a plane ($\kappa^2 = \mu$). For $\xi_2 \leq 2.5$, the ion front is a small pointed projection.

The picosecond and femtosecond laser ablation[1], the ultrafast diagnostics of hydrodynamics [2], the laser-ion acceleration[3], etc., attract more and more international attention since the great development of ultrashort and ultraintense laser technologies. The theory of plasma expansions is not only the fundamental mechanism of laser ablation but also the laser-ion acceleration. Although various theory such as phase explosion [4], Coulomb explosion [5], self-similar plasma expansions [6, 7], two-dimension self-similar plasma expansions [8], and a relativistic model[9] have been proposed, the observed angular-ion distributions such as ring structure [10], time-resolved elliptic shadowgraphs of material ejection [1] and coronal hydrodynamics of laser-produced plasma[2] have not been explained analytically. The problems are that: the electrons generated in the laser-solid interactions are anisotropic generally, however the self-similar expansion [6, 7] and the relativistic model are both one-dimension, the two-dimension theory is only valid for a plasma with isotropic pressure, therefore, they can not predict the shapes of plasma front with anisotropic pressure.

In this letter, a self similar two-dimension solution for a plasma expansion with anisotropic pressure is obtained. Although isothermal-expansion assumption is used, the solution is still suitable for a system whose temperature changes slowly, since the whole process can be separated to several periods and the temperature can be assumed as a constant in any period. In the solution, there are two important parameters: the ratio of the longitudinal temperature, T_{\perp} and the transverse temperature, T_{\parallel} of the plasma, $\kappa^2 = T_{\perp}/T_{\parallel}$, and the electron-ion mass ratio, $\mu = Zm_e/m_i$, where Z is the charge number of the ion, $m_e(m_i)$ is the electron (ion) mass. With the solution, it is found that the relationship between κ^2 and μ decides the shape of the ion front: a complicated surface or an ellipse shown by Figure 1. For $\kappa^2 \in [0, \mu)$, the ion front is composed by a part of a hyperbolic and a small pointed projection at the center. In the critical case, $\kappa^2 = \mu$, the ion front is a plane and a small pointed projection at the center. For $\kappa^2 \in (\mu, 1]$, the ion front is a part of an ellipse and the major axis is in the lower-temperature axis. The ion velocity at the ion front has the similar construction to that of the ion front. However, for $\kappa^2 \in (0, 1)$, the major axis of the ion-velocity ellipse is in the higher-temperature axis. The difference of the angular-energy distribution from the known one[8, 11] is that the energy is a delta function at the maximum angle of near 90° for $\kappa^2 \leq \mu$. It is an anomalous high-energy plasma emission at the angle of near 90° due to the longitudinal Coulomb explosion. The plasma expansion is adiabatic and the temperature changes slowly in a vacuum. However, there is energy transmission from the plasma to the air besides that between the two directions of the plasma. With the assumption: the plasma temperature decreases with time exponentially in the air[12], the dependence of the position of the ion front in the central axis on time is compared with that observed by Zhang and coworkers's in [1]. From the comparison, it is inferred that the plasma front shown in [1] should be the front of Al^+ , Al^{2+} or Al^{3+} .

We assume the pressure tensor of a two-dimension anisotropic plasma satisfies :

$$\overleftrightarrow{P} = \begin{pmatrix} n_e k_B T_{\parallel} & 0 \\ 0 & n_e k_B T_{\perp} \end{pmatrix}. \quad (1)$$

if the ion temperature $k_B T_i \ll k_B T_{\parallel}$ and $k_B T_i \ll k_B T_{\perp}$, where T_{\parallel} is the electron temperature in the x direction and T_{\perp} is the electron temperature in the y direction which is perpendicular to x. In the following discussion, we will show the importance of the ratio, T_{\perp}/T_{\parallel} , and the dependence of the shape of the plasma front on the ratio. In the calculation of the formula of the ion front, we assume the plasma expansion is isothermal. However, if the temperature changes with time slowly, in any interval short enough, the temperature can also be considered as a constant and our calculation and results still hold. Therefore, to a certain extent, our calculation and results allow a wide latitude of

generality in applications.

For convenience, the physical parameters: the time, t , the length coordinate, $x(y)$, the ion (electron) velocity, $v_i(v_e)$, the electron field, E , and the ion (electron) density, $n_i(n_e)$ are normalized by the inverse of the equivalent plasma frequency, $\omega_{pi0} = \sqrt{n_{e0}e^2/m_i\epsilon_0}$, the equivalent plasma Debye length, $\lambda_{D0} = c_s/\omega_{pi0}$, the equivalent ion acoustic speed, $c_s = \sqrt{Zk_B T_e/m_i}$, $E_0 = k_B T_e/e\lambda_{D0}$, and the reference hot-electron density, n_{e0} respectively, where m_i is the ion mass, Z is the charge number of the ion, e is the elemental charge and $T_e = T_{\parallel} + T_{\perp}$ is an equivalent temperature. Then the electric potential is normalized as $\phi = e\psi/k_B T_e$, where ψ is the physical potential. $t, x(y), v_i(v_e), E, n_i(n_e)$ are still used to represent the normalized parameters in the following discussion.

In the new frame: $\tau = t, \xi_1 = x/R_1(t), \xi_2 = y/R_2(t)$, the ion (electron) velocity[8] satisfies: $v_{i,x}(v_{e,x}) = \xi_1 R_1', v_{i,y}(v_{e,y}) = \xi_2 R_2'$. The ion (electron) density is assumed as: $n_{i(e)} = N_{i(e),1}(\xi_1, \xi_2)/R_1^2 + N_{i(e),2}(\xi_1, \xi_2)/R_2^2$, which is similar to that in [8]. With the transformation, the equations of continuity and motion, and Poisson's equation are obtained easily in the new coordinate system. The condition for the automatical satisfiability of the continuity equation is $R_2/R_1 = \kappa$, where κ is a constant. Then the ion (electron) density is simplified to $N_{i(e)}(\xi_1, \xi_2)/R^2(t)$, where $N_{i(e)} = N_{i(e),1} + N_{i(e),2}/\kappa^2$, $R = R_1$. Solving the new motion equation of ions gives the potential in the ion region, $\phi = -\phi^0(\xi_1^2 + \kappa^2 \xi_2^2)$, where ϕ^0 is a constant. Therefore the electron density in the ion region satisfies: $N_e(\xi_1, \xi_2) = N_{e,0} \exp[-(1 + \mu)\phi^0(\xi_1^2 + \xi_2^2)/\alpha_1]$ by solving the electron motion equation with $\kappa^2 = T_{\perp}/T_{\parallel}$, where $\alpha_1 = T_{\parallel}/T_e$. From Poisson's equation, the ion density is $N_i = N_e + 4$. The electron motion equation can be solved in the ion region due to the special form of the electric potential: $\phi = \phi_1(\xi_1) + \phi_2(\xi_2)$. However, beyond the ion front, the potential and electron density are governed by the motion equation of electrons and Poisson's equation together, since the potential can not be separated to $\phi_1(\xi_1) + \phi_2(\xi_2)$ and then the electron density can not be solved from the motion equation solely. Combined the motion equation and Poisson's equation, a two-order partial differential equation of the electron density can be achieved. The first integral of it gives: $(\frac{\partial Y}{\partial \xi_1})^2 + \kappa^2 (\frac{\partial Y}{\partial \xi_2})^2 = \frac{2 \exp(Y) - 4(1 + \kappa^2)\mu\phi^0 Y}{\alpha_1} + C_0$, where C_0 is the first integral constant and $Y = \ln(N_e)$. The physical condition requires that Y is a C^1 function and therefore, the curve equation of the ion front is:

$$\frac{\xi_1^2}{A^2} + \frac{\xi_2^2}{B^2} = D \exp[-\frac{(\xi_1^2 + \xi_2^2)}{2D\phi^0}] + C_0. \quad (2)$$

$$A^{-2} = 1 - \mu\kappa^2, B^{-2} = \kappa^2 - \mu, D = \frac{1}{2(1+\mu)(1+\kappa^2)\phi^{0,2}}.$$

where C_0 is a constant and $\phi^{0,2}$ is the square of ϕ^0 . With Eq. (2), the curve of the ion front may be

some part of a hyperbola, an ellipse or a cycle approximately for different ratio of the temperatures (T_{\perp} and T_{\parallel}), κ^2 . A critical value of κ^2 is the mass ratio of electron and ion, μ or the inverse of it.

Due to the assumed symmetrical form of the pressure, we just need to consider the cases for $\kappa^2 = T_{\perp}/T_{\parallel} \in [0, 1]$. Figure 1 shows the eight cases of the ion front for $\kappa^2 \in [0, 1]$, which are obtained by solving Eq. (2) with $C_0 = 0$ and $\phi^0 = 1$. For $\kappa^2 > \mu$, the curve of the ion front is a part of an ellipse whose eccentricity is $e = \frac{(1-\kappa^2)(1+\mu)}{1-\kappa^2\mu}$ as shown by Fig. 1(a). As $\kappa^2 \rightarrow \mu$, $e \rightarrow 1$. Specially, for $\kappa^2 = 1$, i.e., $T_{\perp} = T_{\parallel}$, the ion front is a part of a cycle. For $\kappa^2 \leq \mu$, the ion front is complicated and contains two parts: a part of a hyperbola and another curve as shown by Fig. 1(b). For the part of the hyperbola, $\xi_2 \geq 2.5$ and the slope of the asymptote is $\sqrt{\frac{1-\mu\kappa^2}{\mu-\kappa^2}}$. As $\kappa^2 \rightarrow \mu$, the slope trends to infinite and the ion front becomes a flat surface as shown by the dash dot line in Fig. 1(b).

Now imaging the following physical picture: the initial state is $T_{\perp,0} = \mu T_{\parallel,0}$, and the temperature T_{\perp} increases slowly to the equilibrium temperature, T_{eq} (Note: $T_{eq} = (\mu + 1)T_{\parallel,0}/2$ in our two dimensional case. However, in the three dimensional case, if we assume the temperature in the y direction is equal to that in the z direction at the very beginning time, $T_{eq} = (2\mu + 1)T_{\parallel,0}/3$), when the thermodynamic equilibrium is reached, since the energy is transmitted between the transverse direction x and the longitudinal directions (Note: in two dimensional case, y or z is the longitudinal direction; in the three dimensional case, y and z are all longitudinal directions where we assume the temperature in the y direction is equal to that in the z direction.) with collisions. At the very beginning time, the ion front is a flat surface with a small pointed projection at the center shown by the dash dot line in Fig. 1(b). After an interval, $\kappa^2 > \mu$, and then the ion front develops to a part of ellipses shown by the solid, dash, and dot line step by step in Fig. 1(a), which are also shown by Figure 2 (b-h) in [1]. At last, the ion front trends to a part of a cycle shown by the dash dot line in Fig. 1(a), which is also shown by outer layer of Figure 2(i) in [1]. That is a depiction of the two dimensional plasma expansion into a vacuum. However, it has not been verified experimentally in a vacuum. In spite of that, the time-resolved shadowgraphs of material ejection shown by Zhang and coworkers in [1] support our theory without doubt. The outermost layer of the shadowgraph does undergo the physical processes depicted by our above discussion. It is the most difference between the experiment and our scene that the plasma expansion is in the air or in a vacuum. In the air, there are thermal transmission from the plasma to the air, collisions between the plasma and the air molecules and other nonlinear effects, and then the outermost layer of the plasma cools down. In this case, the shock wave front (shown by Fig. 3 in [1]) forms since the particles inner the

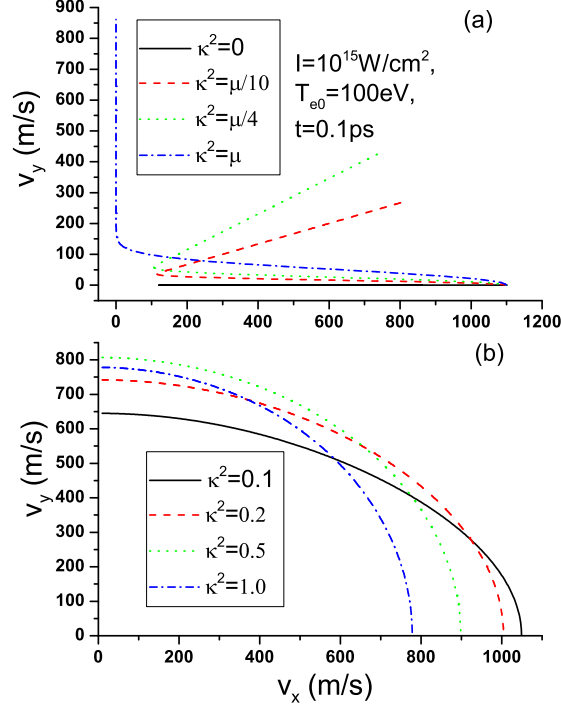


FIG. 2: (Color online) The ion velocity distribution at the ion front for $I = 10^{15} \text{ W/cm}^2$, $\lambda = 0.8 \text{ nm}$, and $\kappa^2 = T_{\perp}/T_{\parallel} \in [0, 1]$, $\phi^0 = 1$ in Eq. (2), $\alpha(t) = 0.003$ at $t = 0.1 \text{ ps}$. (a) The ion velocity distribution at the ion front for $\kappa^2 \leq \mu$. (b) The ion velocity distribution at the ion front for $\kappa^2 > \mu$.

plasma catch up with the particles at the front. In a vacuum, these phenomenons can not happen.

With the ion motion equation, $R(t)$ satisfies: $\int_0^{\alpha} \exp(\alpha_1^2) d\alpha_1 = \sqrt{\phi^0 t}/R_0$, where $\alpha = \sqrt{\ln(R/R_0)}$ and $R_0 = R(t = 0)$. Figure 2 shows the ion-velocity distribution at the ion front obtained from our two-dimension theory for different temperature ratio, $\kappa^2 = T_{\perp}/T_{\parallel} \in [0, 1]$. For different times, the shapes of the ion-velocity distribution are the same although the amplitudes are different. For $\kappa^2 \in (0, \mu)$, the velocity distribution has two parts: ellipse-like at small v_2 and hyperbolic-like at large v_2 , which is shown by the dot line or the dash line in Fig. 2(a). The solid line in Fig. 2(a) shows all the ions move towards the x direction since the temperature in the y direction is zero. The dash dot line in Fig. 2(a) shows the critical case: $\kappa^2 = \mu$, in which the velocity in the x direction at large v_2 is zero and all the ions move in the y direction. For $\kappa^2 \in (\mu, 1]$, the ion velocity distribution is a part of an ellipse whose eccentricity is $\sqrt{\mu(\kappa^{-2} - \kappa^2)}/(1 - \mu\kappa^{-2})$ and the major axis is in the high temperature direction, x. At $\kappa^2 = 1$, the ion-velocity distribution is a part of a cycle and isotropic as shown by the dash dot line in Fig. 2(b).

Figure 3 shows the angular-energy distribution for $\kappa^2 \in [0, 1]$. With it, the facts are indicated

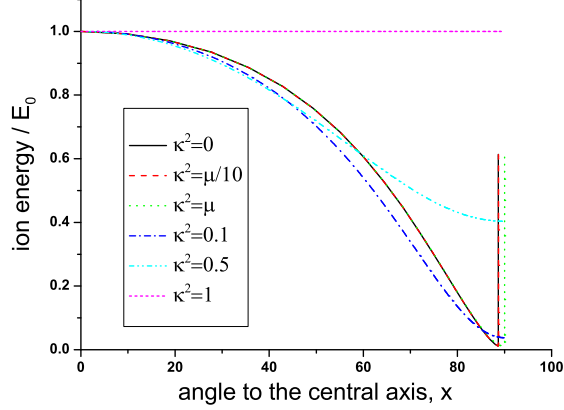


FIG. 3: (Color online) The ion energy distribution at the ion front VS the angle to the central axis, x , for $\kappa^2 = T_{\perp}/T_{\parallel} \in [0, 1]$, $\phi^0 = 1$ in Eq. (2). In this figure, the energy for any angle is normalized by E_0 for each κ^2 , where E_0 is the ion energy at the central axis.

: (1) for $\kappa^2 \in [0, \mu]$, the energy decreases with angle except for the maximum angle of near 90° . At the maximum angle, the energy is a delta function with the peak value of about $0.62E_0$. Especially, the maximum angle is 90° for the critical point, $\kappa^2 = \mu$. This anomalous plasma emission happens since the large Coulomb space-charge field dominates in the longitudinal direction and is counteracted partly by the gradient of the pressure in the transverse direction. (2) for $\kappa^2 \in (\mu, 1)$, the ion energy decreases with angle monotonously. At $\kappa^2 = 1$, the energy is a constant function with respect to angle.

As discussed above, there is energy transmission from the plasma to the air for plasma expansions in the air. Therefore, besides the energy transmission between the longitudinal direction and the transverse direction of the plasma, the temperature of the plasma decreases exponentially to zero for the time long enough since the temperature of the air is about 0eV. As an important application, the position of the ion front in the air can be given by our solution with the assumption: the temperature, T_e decreases exponentially to zero[12] with the scale time of the temperature, $t_{eff} = -\partial \ln(T_e)/\partial t$. Therefore $T_e = T_{e0} \exp(-t/t_{eff})$ in the air and $T_e = T_{e0}$ (which is $(T_{\perp 0} + T_{\parallel 0})$ in the two dimensional case and $(2T_{\perp 0} + T_{\parallel 0})$ in the three dimensional case where the longitudinal temperatures are the same.) in a vacuum. The ions at the outermost layer are decelerated for the plasma expansion in the air after a period of time shown by the dash line and the dash dot line in Figure 4(a), however, the velocity of them tends to a constant in a vacuum shown by the dash line and the dot line in Figure 4(a).

Figure 4(a) shows different ion fronts in a vacuum, in the air and for different initial charge-

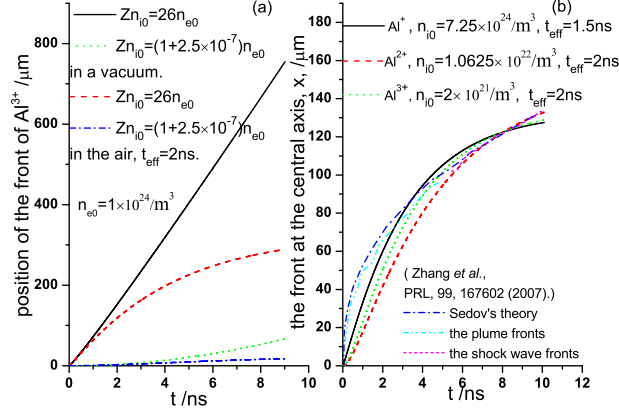


FIG. 4: (Color online) (a) The ion front of Al^{3+} in the central axis, x , with $\xi_{1,f} = 0.42, \xi_{2,f} = 0$, VS t , for $n_{e0} = 10^{24}/\text{m}^3$, and $Zn_{i0} = 26n_{e0}$, shown by the solid line (in a vacuum) and the dash line (in the air, with the scale time of temperature, $t_{eff} = 2\text{ns}$), and $Zn_{i0} = (1 + 2.5 \times 10^{-7})n_{e0}$, shown by the dot line (in a vacuum) and the dash dot line (in the air, with the scale time of temperature, $t_{eff} = 2\text{ns}$); (b) the front of different ions in the central axis, x , with $\xi_{1,f} = 0.42, \xi_{2,f} = 0$, VS t . The solid line, the dash line and the dot line correspond to the expansion in the air and are obtained by our solution. The solid line is for Al^+ , and $Zn_{i0} = 7.25n_{e0}, t_{eff} = 1.5\text{ns}$. The dash line is for Al^{2+} , and $Zn_{i0} = 1.0625n_{e0}, t_{eff} = 2\text{ns}$. The dot line is for Al^{3+} , and $Zn_{i0} = 2n_{e0}, t_{eff} = 2\text{ns}$. The dash dot line, the dash dot dot line, the short dash line correspond to Figure 4 in [1].

separation densities. The difference of the ion fronts in a vacuum and in the air has been discussed in the above paragraph. In the air, the collisions between the plasma and the air molecules are important for the expansion and considered gracefully through the exponential decrease of the plasma temperature. The collisions result in nonlinear phenomena and energy transmission. For different initial charge-separation densities of the plasma, the stronger the initial charge-separation field and the more efficient the ions are accelerated as shown by the comparison between the solid line and the dot line or between the dash line and the dash dot line in Fig. 4(a). When an ultra-short and ultra-intense laser pulse interacts with a solid target, many interesting phenomena: hot-electrons generation and acceleration, x-ray and γ -ray emission, fast ions generation, plasma ablation and plasma splash and so on occur. For different phenomena, the scale time is different. A fact is: the smaller the scale time, the stronger the charge-separation field and the nonlinearity in parameters of the plasma. For the generation of fast ions, the scale time is about 1 – 10ps. However, for the laser-plasma ablation, the scale time is several nanoseconds or even longer. In the

period of several pulse durations, the charge-separation field is strong, i.e., the density difference, $Zn_i - n_e$ (which is $4/R^2$ here.) is large (since $R(t)$ increases with time and tends to infinite as $t \rightarrow +\infty$). Therefore, with the self-similar solution for energetic ions generation given by Huang and coworkers' in [7], the high charge-mass ratio, Z/M , ions are accelerated preferentially and efficiently. When an ultra-intense laser pulse interacts with a solid target, H^+ , C^{4+} , C^{3+} , O^{4+} and so on are accelerated orderly. For Al target, Al^{3+} , Al^{2+} , Al^+ are accelerated lastly. According to our analysis, the front surface observed by Zhang and coworkers' in [1] should be the ions of Al and the density of the ions should be low since the scale time is of nanoseconds. The fronts of the ions: Al^{3+} , Al^{2+} , Al^+ in the central axis, x , with $\xi_{1,f} = 0.42$, $\xi_{2,f} = 0$ are calculated and compared with the curves given by Zhang and coworkers' in [1] as shown by Figure 4 (b). They are consistent.

In conclusion, the analytic solution for the ion front of plasma expansion with anisotropic pressure is predicted. It is supported by experiments[1, 2] lately. The ion-velocity distribution at the ion front, angular-energy distribution at the ion front are both given. It needs to be concerned that the energy is a delta function at the maximum angle of near 90° and the plasma emits anomalously due to the longitudinal coulomb explosion for $\kappa^2 \in [0, \mu]$ as shown by the solid, dash, dot lines in Fig. 3. In a vacuum, the expansion is adiabatic, however, in the air, the temperature decreases with time exponentially and collisions happen, and then the ions at the outermost layer are decelerated and shock waves generate in the front of the plasma front. From the comparison (shown by Fig. 4), it is concluded that the ions observed in [1] are the ions of Al. However, the collisions and the nonsymmetric components of the pressure tensor of plasmas have not been considered directly in the calculation. Therefore, how the energy transmission between the longitudinal direction and the transverse direction or between the plasma and the air can not be described in detail. In the air, they are challenges for our future work.

This work was supported by the Key Project of Chinese National Programs for Fundamental Research (973 Program) under contract No. 2006CB806004 and the Chinese National Natural Science Foundation under contract No. 10334110.

[1] N. Zhang, X. Zhu, J. Yang, X. Wang, and M. Wang, Phys. Rev. Lett. 99, 167602 (2007).

[2] A. Aliverdiev *et al.*, Phys. Rew. E 78, 046404 (2008).

[3] H. Schwoerer *et al.*, Nature 439, 445 (2006);

- [4] P. Lorazo, L. J. Lewis , and M. Meunier, Phys. Rev. Lett. 91, 225502 (2003).
- [5] W. G. Roeterdink *et al.*, Appl. Phys. Lett. 82, 4190 (2003).
- [6] P. Mora, Phys. Rev. Lett. 90, 185002 (2003).
- [7] Y. S. Huang *et al.*, Appl. Phys. Lett. 92, 031501 (2008).
- [8] Y. S. Huang *et al.*, Appl. Phys. Lett. 92, 141502 (2008).
- [9] M. Passoni and M. Lontano, Phys. Rev. Lett. 101, 115001 (2008).
- [10] E. L. Clark *et al.*, Phys. Rev. Lett. 84, 670 (2000);
- [11] R. A. Snavely *et al.*, Phys. Rev. Lett 85,2945(2000);
- [12] X. Wang and X. Xu, Journal of Thermal Stresses 25, 457 (2002).